Technical Note

Functional MRI of the Thoracic Spinal Cord During Vibration Sensation

Jennifer Kornelsen, PhD,[1,2]* Stephen D. Smith, PhD,[1,2] Theresa A. McIver, BAH,[1,2] Uta Sboto-Frankenstein, PhD,[1] Peter Latta, PhD,[1] and Boguslaw Tomanek, PhD[1]

Purpose: To demonstrate that it is possible to acquire accurate functional magnetic resonance images from thoracic spinal cord neurons.

Materials and Methods: The lower thoracic spinal dermatomes (T7–T11) on the right side of the body were mechanically stimulated by vibration for 15 participants. Neuronal responses to vibration sensation were measured in the thoracic spinal cord using a HASTE sequence on a 3 Tesla MRI system.

Results: Signal increases were observed in the corresponding lower thoracic spinal cord segments ipsilateral to the side of stimulation in the dorsal aspect of the spinal cord.

Conclusion: This is the first study to provide proof of principle that functional imaging of the entire thoracic spinal cord is possible, by detecting neuronal activity in the thoracic spinal cord during sensory stimulation using spinal fMRI.

Key Words: spinal cord; functional magnetic resonance imaging; thoracic; vibration; sensory
J. Magn. Reson. Imaging 2013;37:981–985.

THE USE OF functional MRI (fMRI) for examining neural activity in the spinal cord (spinal fMRI) has been growing over the past decade (1). Studies using spinal fMRI have identified neuronal activity related to both sensory and motor function. Although most of these studies have focused on functional activity in the cervical spinal cord immediately below the brainstem (2–6), other research has accurately detected activations in the lumbar spinal cord (7). However, to date, no studies have focused on signal detection in the thoracic spinal cord, the region that connects the cervical and lumbar regions. This paucity of data is due to several specific challenges related to imaging the thoracic spinal cord. For example, in all spinal fMRI the heterogeneous tissue surrounding the spinal cord makes signal detection difficult (8), cardiac-related noise and respiratory movement can cause artifacts (4) and subject or task-related movement can contaminate the data. Specific to the current study, the diameter of the thoracic spinal cord is quite narrow, even when compared with other spinal cord segments (9). Therefore, successful imaging of this region would serve as an invaluable technical advancement, and would allow researchers to further delineate the functions served by this region of the central nervous system.

To provide an initial proof-of-principle for functional MRI of the thoracic spinal cord, it is necessary to demonstrate that the pattern of activation in response to simple stimuli is consistent with the neuronal afferents identified in neuroanatomical studies. Vibration stimulation of the torso is an appropriate sensory stimulus as it can be applied to the dermatomes that correspond to the lower thoracic spinal cord segments, unilaterally. Indeed, vibration stimuli were used in earlier studies to elicit activation of the cervical and lumbar spinal cord (10). Vibration can occur at low (less than 50 Hz) or high frequencies (above 50 Hz). During low-frequency vibration, Meissner's corpuscles in the skin are activated and convey information to several parallel ascending sensory tracts, including the dorsal column-medial lemniscus pathway, the spinocervical tract and spinothalamic tract (11). During high-frequency vibration, Pacinian corpuscles in the skin are activated and convey information by means of the dorsal column-medial lemniscus pathway. This pathway consists of large-diameter myelinated afferent nerves that travel in the dorsal funiculus (12). The fibers that innervate the lower torso ascend in the gracile fasciculus to the gracile nuclei in the medulla. In the current study, we applied a vibration stimulus by means of a 5 × 13 cm device at 50 Hz to the T7 through T11 spinal cord dermatomes on the lateral aspect of the right side of the torso. This frequency stimulates both the low- and high-frequency systems, although identification of these two

[1]National Research Council Institute for Biodiagnostics, Winnipeg, Manitoba, Canada.
[2]Department of Psychology, University of Winnipeg, Winnipeg, Manitoba, Canada.
Contract grant sponsors: Manitoba Medical Service Foundation; the Natural Sciences and Engineering Research Council of Canada.
*Address reprint requests to: J.K., National Research Council Institute for Biodiagnostics, 435 Ellice Avenue, Winnipeg, MB, Canada R3B 1Y6. E-mail: jennifer.kornelsen@nrc-cnrc.gc.ca
Received June 24, 2011; Accepted August 14, 2012.
DOI 10.1002/jmri.23819
View this article online at wileyonlinelibrary.com.

separate pathways is not anticipated. Our aim in using this frequency was to increase the likelihood of detecting a neuronal response to the sensory stimulus during this initial attempt to image the thoracic spinal cord. We hypothesized that a neuronal response, indicated by active voxels, would be elicited ipsilateral to the side of the body stimulated, in the dorsal (sensory) horns of the corresponding lower thoracic spinal cord segments (T7–T11).

MATERIALS AND METHODS

Participants

Fifteen healthy right-handed undergraduate university students participated in this study (8 female, age range = 18–25 years, mean age = 20.9). All participants underwent MR screening to ensure that they could be safely scanned. Ethical approval was obtained from our institutions' Human Research Ethics Boards. All participants provided written informed consent before their participation in these studies.

Stimulus Materials and Paradigm

The vibration sensation was generated with an MR-compatible custom-built actuator (13). The actuator probe had an approximately 5 × 13 cm contact area with the body and was set to vibrate at 50 Hz. The vibration was applied to the T7 through T11 spinal cord dermatomes on the lateral aspect of the right side of the torso. The vibration stimulation was set to vibrate in a block paradigm of 40-s rest and 60-s stimulation blocks, repeated three times for a total functional scan time of 340 s. Each participant completed this paradigm twice.

MR Methodology

Experiments were conducted with a 3.0 Tesla (T) Siemens Magnetom Trio TIM system. A Siemens RF body coil was used for excitation and a Siemens Spine Matrix was used for reception. Spinal cord fMRI was performed using a single shot fast spin-echo sequence with partial Fourier sampling (HASTE) with a TE = 38 ms and a TR = 1000 ms per slice (14). Seven 2-mm-thick contiguous sagittal slices were acquired with the following acquisition parameters: flip angle = 125°, 195 Hz/pixel bandwidth, 90 × 128 matrix size, echo spacing = 9.68 ms, FOV = 200 × 100 mm, 50% phase encode FOV. Slices were centered rostro-caudally on the T5 vertebra and spanned the thoracic spinal cord segments. Spatial saturation pulses were applied to eliminate signal from surrounding areas to avoid aliasing and to reduce motion artifacts arising from regions anterior to the spine.

Data Analysis

Data were preprocessed and analyzed with Matlab custom written software (Mathworks, Inc., Natick, MA). Three series of data were removed from the analysis. Two runs from one participant were removed due to excessive blurring on one series and incompletion of the second series, and one series from another participant was removed due to excessive blurring and movement of the subject's spinal cord out of the field of view. This resulted in 27 usable data series. To realign each spinal fMRI data series, a raw data image was used to define the location and curvature of the spinal cord, according to established spinal fMRI data analysis methodology (15). A reference line was drawn manually along the anterior edge of the spinal cord in the sagittal plane and the C7/T1 and T8/T9 intervertebral disks were marked. The data at each time point were combined into a three-dimensional volume and were linearly interpolated to 0.5-mm cubic voxels. The volume was then resliced transverse to the manually drawn reference line. The reference line was used to realign the slice data to correct for motion between time points and to apply spatial smoothing in the rostro-caudal direction. Each series was analyzed using the general linear model as described in previous research (15) with the basis set generated for the stimulation paradigm described above, consisting of a block paradigm of a 40-s rest before and after each 60-s block of stimulus presentation, with baseline calculated as the mean intensity during rest. Consistent with previous published work (16), a threshold of t = 2.0 (Bonferroni corrected for multiple comparisons at $P = 0.05$) was chosen to identify active voxels for display in color on a gray-scale reference image. The analyzed individual results were then spatially normalized by reslicing the spinal cord every 1 mm along the length of the reference line between the C7/T1 and T8/T9 discs and by scaling to a 140 mm length and fine-tuning the alignment in each transverse slice. A random effects analysis was conducted and activity maps of the significantly activated voxels ($P = 0.003$) were created for the group. The signal intensity of the active voxels was used to produce a graph of the intensity changes across volumes during the study to aid in visualizing the correspondence of the changes in signal intensity with the study paradigm.

RESULTS

The vibration stimulus elicited activations in all analyzed experimental runs for all subjects. In the grouped analysis for each run, the activity was observed in the lower thoracic spinal cord segments which correspond to the level of the stimulus presentation. In the grouped analysis of the first run for all participants, the activity occurred in the medial and right dorsal T8 and medial dorsal T11 spinal cord segments. In the second run for all participants, the activity occurred in the right dorsal T7, right dorsal T8, medial and right dorsal T9, right dorsal T10, right lateral and left dorsal T11, and right dorsal and lateral T12 spinal cord segments.

A grouped analysis of both runs from all participants shows the location of consistently occurring activity across all participants (see Fig. 1). Activity

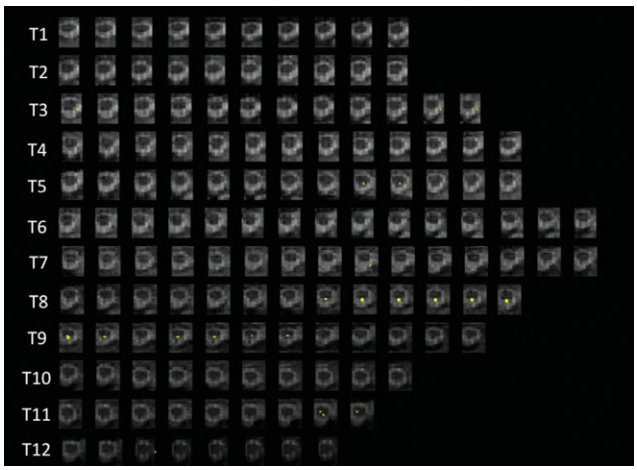

Figure 1. Axial slices spanning the thoracic spinal cord segments for all data in a random effects analysis. The thoracic spinal cord was spatially normalized to a length of 140 mm. Axial slices were obtained by reslicing transverse to the spinal cord at 1-mm intervals and are shown here in the number of 1-mm slices that each thoracic spinal cord segment would occupy following normalization, as indicated on the left. Images are displayed from rostral to caudal from left to right in each row, with the dorsal side of the cord toward the bottom of each frame, and the left side of the cord to the right of each frame (radiological convention). Activity (P = 0.003) can be observed in the medial and right dorsal T8, T9, and T11 spinal cord segments.

occurred in the medial and right dorsal aspect of the spinal cord, consistent with neuronal input from sensory afferents. The activity was observed in the T8, T9, and T11 spinal cord segments. The grouped analysis map was converted to sagittal orientation for display (see Fig. 2).

The average signal intensity was 6.88%, consistent with previously reported values. The time course for the signal intensity data shows congruence with the stimulation paradigm (see Fig. 3).

DISCUSSION

The current research demonstrates that functional MRI can reliably detect signal intensity changes associated with sensory functions in the thoracic spinal cord. Activity occurred in the medial and right dorsal aspect of the spinal cord, consistent with neuronal input from sensory afferents. The activity occurred on the right side of the spinal cord, which is consistent with the presentation of the vibration stimulus. Our reported signal intensity of 6.88% is also consistent with that reported in the literature for spinal fMRI studies using similar sequences and parameters (e.g., 6, 7, 10). The time course of the signal change shown in Figure 3 further supports our claim that the activity observed is related to the presentation of the vibration stimulus. The measured signal time course closely follows that of the stimulation paradigm. Taken together, the agreement of the location of activity with the placement of the stimulus on the dermatomal map, the appropriate signal intensity value, and the correspondence of the time course data with the stimulation paradigm, strongly supports the efficacy of fMRI measurements in detecting signal intensity changes related to neuronal activity in the thoracic spinal cord.

The results of our study are in agreement with those of a previous spinal cord fMRI study using vibration stimulation of the cervical and lumbar spinal cord segments; in that study, activity was observed in the spinal cord segments that corresponded to five different noncontinuous dermatomes that were stimulated (10). The current study also involved five-dermatome stimulation. We did not attempt to stimulate a single dermatome with our device because there is such great overlap in the boundaries of segments that it would be unreasonable to expect a unique response from a precise spinal cord segment. Additionally, as this study was an initial demonstration of the feasibility of imaging the thoracic spinal cord, we elected to use a prominent stimulus likely to elicit a detectable response. However, because we have identified the region of the spinal cord that matches with the stimulated dermatomes with a high degree of statistical significance, and given the absence of activity elsewhere in the cord, we can be confident that our distribution of activity is due to the vibration sensation.

Although previous spinal fMRI studies using vibration did not identify distinct patterns of lateralization, such patterns were observed in the current study. This difference is likely due to slightly different scanning parameters which enhanced the precision of our imaging. An advantage of the methodology in the current study was the use of the sagittal image

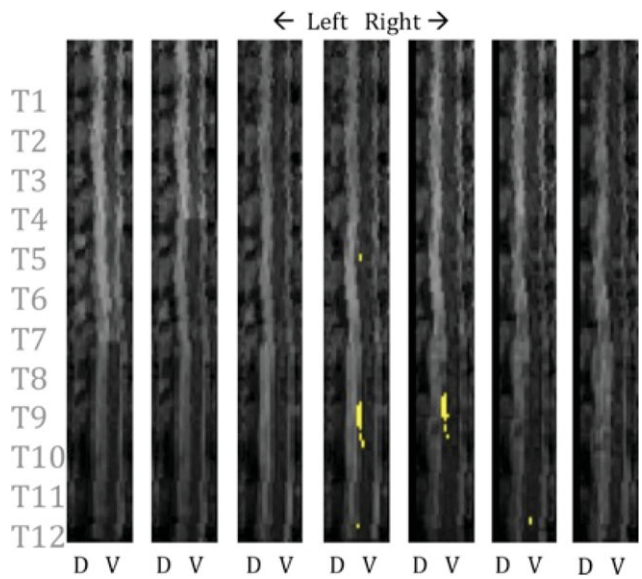

Figure 2. Sagittal slices spanning the thoracic spinal cord segments for all data in a grouped analysis. Activity (P = 0.003) can be observed in the slices in the center and to the right of center in the lower thoracic spinal cord, T8 to T11. Slices are displayed rostral to caudal from the top to bottom of each frame, with the slices taken from the left side to the right side of the spinal cord as labeled, and with dorsal (D) to the left and ventral (V) to the right of each frame. Approximate thoracic spinal cord levels are indicated on the left.

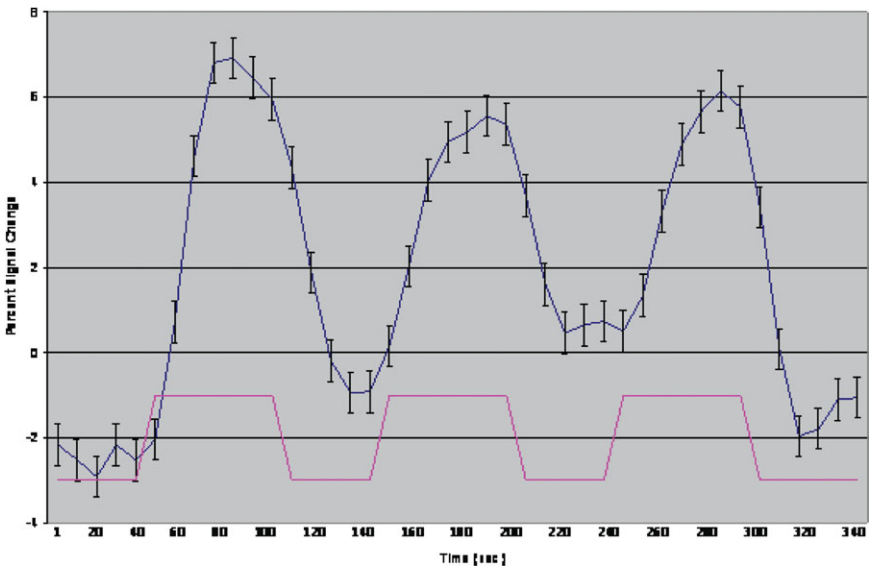

Figure 3. The time course of the signal intensity (with standard error bars) of all active voxels identified with the random analysis for all subjects across time (seconds) is shown. The correspondence of the changes in signal intensity (blue line) and the stimulation paradigm (pink line) is observable. [Color figure can be viewed in the online issue, which is available at wileyonlinelibrary.com.]

acquisition technique, which allowed for a greater rostral-caudal range of the spinal cord to be acquired. As the resulting activity maps are shown in both axial and sagittal orientation, it is possible to determine where the activity occurs both in cross-section and along the length of the thoracic spinal cord.

The scanning parameters used in the current study typically produce high image quality and spatial resolution and have a reduced sensitivity to magnetic field distortions, thus making it a valid measure of spinal cord activity (8). The single shot fast spin-echo sequence with partial Fourier sampling (HASTE) has a short TE and long TR. Previous research has shown that at short echo times, spin echo sequences detect signal changes resulting from proton density changes associated with cellular swelling, termed 'signal enhancement by extravascular water protons' or 'SEEP' (14). Therefore, the current scanning sequence assesses neural activity in a manner similar to proton-density-weighted imaging. In addition to these pulse sequence advantages, we applied a saturation band to eliminate signal anterior to the spine from the heart and lungs. We have also used a sensory stimulus that produces very little movement of the subject during stimulation, thus limiting the potential for artifacts. Finally, we have used a previously established analysis methodology that aligns and smoothes across tissues rostro-caudally to avoid partial volume effects. Together, these methodological and analysis techniques were sufficient for detection of activity in the thoracic spinal cord.

The ability to measure functional activity in the thoracic spinal cord using fMRI will greatly benefit spinal cord research. Through the use of this noninvasive technique, it is possible to answer basic science questions regarding thoracic spinal cord function; it will also be possible to assess autonomic nervous system activity, as several components of this system synapse in the thoracic spinal cord (17). In addition, this advancement bridges the gap between functional imaging of the previously established cervical and lumbar spinal cord. This ability to image the entire spinal cord would be useful for the diagnosis and possible rehabilitation of spinal cord injuries and of neurodegenerative disorders such as multiple sclerosis. Currently, vibration stimulation with cotton balls is used to assess light-touch sensation in patients with spinal cord injuries. Using spinal fMRI during vibration stimulation as an additional diagnostic and/or treatment-evaluation test would allow physicians to *quantify* patients' neural responses, thereby providing a more accurate depiction of preserved spinal cord functioning. Such measurements would also allow physicians to measure improvements in functioning during the rehabilitation process.

Although this study indicates that spinal fMRI can be conducted in the thoracic cord with a vibration stimulus, it remains to be seen whether other sensory stimuli or performance of a motor task will elicit reliable responses. Before this technique can be useful clinically, the sensitivity will need to improved on an individual level. The use of retrospective spinal cord motion time-course estimates (18) or physiological noise modeling (19) may be sufficient for this imaging technique to be more sensitive at the individual level. Further adjustments to improve sensitivity might include longer acquisition time with a greater number of volumes acquired and more accurate modeling of the impulse response function for the spinal cord as recently reported in an event-related spinal fMRI study (20). While advances in methodology are necessary to bring spinal fMRI closer to clinical use, numerous important questions still can be addressed with the state of the technology at present.

In conclusion, the results of the current study suggest that it is possible to acquire accurate functional images of activity in the thoracic spinal cord. As fMRI of the cervical and lumbar spinal cord is well-established, thoracic imaging will now allow for noninvasive measurement of functional activity along the entire neuroaxis.

ACKNOWLEDGMENTS

This work was funded by the Manitoba Medical Service Foundation and the Natural Sciences and Engineering Research Council of Canada.

REFERENCES

1. Summers PE, Iannetti GD, Porro CA. Functional exploration of the human spinal cord during voluntary movement and somatosensory stimulation. Magn Reson Imaging 2010;28:1216–1224.
2. Maieron M, Iannetti GD, Bodurka J, Tracey I, Bandettini PA, Porro CA. Functional responses in the human spinal cord during willed motor actions: evidence for side- and rate-dependent activity. J Neurosci 2007;27:4182–4190.
3. Ng MC, Wong KK, Li G, et al. Proton-density-weighted spinal fMRI with sensorimotor stimulation at 0.2 T. Neuroimage 2006; 29:995–999.
4. Piche M, Cohen-Adad J, Nejad MK, et al. Characterization of cardiac-related noise in fMRI of the cervical spinal cord. Magn Reson Imaging 2009;27:300–310.
5. Xie CH, Kong KM, Guan JT, Chen JX, Wu RH. Functional MR imaging of the cervical spinal cord by use of 20Hz functional electrical stimulation to median nerve. Conf Proc IEEE Eng Med Biol Soc 2007;2007:3392–3395.
6. Xie CH, Kong K, Guan J, et al. SSFSE sequence functional MRI of the human cervical spinal cord with complex finger tapping. Eur J Radiol 2009;70:1–6.
7. Kornelsen J, Stroman PW. fMRI of the lumbar spinal cord during a lower limb motor task. Magn Reson Med 2004;52:411–414.
8. Leitch JK, Figley CR, Stroman PW. Applying functional MRI to the spinal cord and brainstem. Magn Reson Imaging 2010;28: 1225–1233.
9. Miller JS, Chiou-Tan F, Zhang H, Taber KH. Sectional neuroanatomy of the lower thoracic spine and chest. J Comput Assist Tomogrogr 2007;31:160–164.
10. Lawrence JM, Stroman PW, Kollias SS. Functional magnetic resonance imaging of the human cervical spinal cord with vibration stimulation of different dermatomes. Neuroradiology 2008;50: 273–280.
11. Vega JA, Garcia-Suarez O, Montano JA, Pardo B, Cobo JM. The Meissner and Pacinian sensory corpuscles revisited new data from the last decade. Microsc Res Tech 2009;72:299–309.
12. Weerakkody NS, Taylor JL, Gandevia SC. The effect of high-frequency cutaneous vibration on different inputs subserving detection of joint movement. Exp Brain Res 2009;197:347–355.
13. Latta P, Gruwel ML, Debergue P, et al. Convertible pneumatic actuator for magnetic resonance elastography of the brain. Magn Reson Imaging 2011;29:147–152.
14. Figley CR, Leitch JK, Patrick PW. In contrast to BOLD: signal enhancement by extravascular water protons as an alternative mechanism of endogenous fMRI signal change. Magn Reson Imaging 2010;28:1234–1243.
15. Stroman PW. Discrimination of errors from neuronal activity in functional MRI of the human spinal cord by means of general linear model analysis. Magn Reson Med 2006;56:452–456.
16. Stroman PW, Kornelsen J, Lawrence J. An improved method for spinal fMRI with large volume coverage of the spinal cord. J Magn Reson Imaging 2005;21:520–526.
17. Karlsson AK. Autonomic dysfunction in spinal cord injury: clinical presentation of symptoms and signs. Prog Brain Res 2006; 152:1–8.
18. Figley CR, Stroman PW. Development and validation of retrospective spinal cord motion time-course estimates (RESPITE) for spin-echo spinal fMRI: improved sensitivity and specificity by means of a motion-compensating general linear model analysis. Neuroimage 2009;44:421–427.
19. Kong Y, Jenkinson M, Andersson J, Tracey I, Brooks JC. Assessment of physiological noise modelling methods for functional imaging of the spinal cord. Neuroimage 2012;60:1538–1549.
20. Figley CR, Stroman P. Measurement and characterization of the human spinal cord SEEP response using event-related spinal fMRI. Magn Reson Imaging 2012;30:471–484.